International Journal of Engineering

Journal Homepage: www.ije.ir

An Improvement on Slot Configuration Structure for a Low-speed Surface-mounted Permanent Magnet Synchronous Generator with a Wound Cable Winding

H. Parivar, S. M. Seyyedbarzegar*, A. Darabi

Department of Electrical Engineering, Shahrood University of Technology, Shahrood, Iran

P A P E R I N F O

Paper history:
Received 13 March 2021
Received in revised form 07 May 2021
Accepted 15 June 2021

Keywords:
Marine Energy Conversion System
Tidal Energy Conversion System
Cross-linked Polyethylene
Finite-element Method
Torque Ripple
Joule Loss

A B S T R A C T

This paper concentrates on low-speed surface-mounted permanent magnet synchronous generator (LS-SMPMSG) electromagnetic design using finite-element (FEM)-based method. The introduced LS-SMPMSG is utilized in marine energy conversion (MEC) and tidal energy conversion (TEC) systems. The main feature of the designed LS-SMPMSG is its ability to generate electrical power in MEC and TEC systems at a low speed of approximately 100 rpm. In the second part, a new slot structure for LS-SMPMSG has been proposed to enhance the LS-SMPMSG performance. The FEM analysis shows that the new slot structure led to reducing the torque ripple and the cogging torque equal to 19.54% and 87.5% respectively. Also, it influenced the LS-SMPMSG Joule losses by 16.1% reduction. Another advantage of the new slot structure of LS-SMPMSG is its easy construction and assembly. The FEM analysis validates the advantages of the proposed structure.

***doi**: 10.5829/ije.2021.34.09c.01*

1. INTRODUCTION

Permanent magnet (PM) machines are used on a large scale, remarkably in the past two decades [1, 2]. Two important factors that have been highlighted in the utilization of PM machines are cost competition and the availability of rare-earth PMs. Throughout the early ten years, relying on vast resources of rare PM materials, China's production began to flourish. Due to these immense resources, the cost of the PM diminished and made it economical to use [3]. Meaningfully, the electrical machine efficacy has been enhanced by introducing and utilizing PMs [4]. Thus, in the last 20 years, not only the cost of magnets has decreased, but also various categorizations of magnets became available [5]. This has made it conceivable to utilize PM machines even in industries suchlike the aircraft industry or the military. In the present circumstances, PMs with a BH_{max} of more than 60 *MG.Oe* are manufactured and marketed by assorted companies [6].

*Corresponding Author Institutional Email: seyyedbarzegar@shahroodut.ac.ir (S. M. Seyyedbarzegar)

With advances in efficiency-oriented applications, the prominence of economical use of resources has originated the need for compact and high-efficiency electromechanical systems. In practical terms, it conveys that conventional electric machines are being substituted by new models. One of the electrical machines which produce electricity from renewable energy resources is PM machines [7]. Owing to the high-power density of PM material, PM machines might have an upper power density and high efficiency through the absence of excitation, magnetization currents, and insignificant rotor losses. Undoubtedly, PM machines play an indispensable assignment in energy production. Ocean energy is one such emerging energies that have originated promising developments in the energy industry. Momentous commercial developments have been initiated in the US, Europe, Asia, and South America over the next 10 to 20 years [8]. Plenty of generators can be utilized in the wave energy conversion (WEC) systems suchlike squirrel cage induction generator (SCIG), synchronous generator (SG), PM synchronous generator (PMSG). Table 1, illustrated the speed extent of the ordinary generator

Please cite this article as: H. Parivar, S. M. Seyyedbarzegar, A. Darabi, An Improvement on Slot Configuration Structure of a Low-speed Surface-mounted Permanent Magnet Synchronous Generator with a Wound Cable Winding, International Journal of Engineering, Transactions C: Aspects Vol. 34, No. 9, (2021) 2045-2052

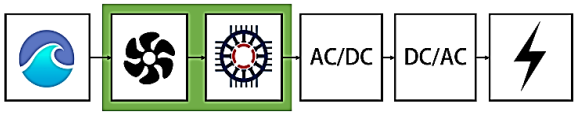

Figure 1. The Wave Energy Conversion (WEC) system

TABLE 1. Generator speed ranges for each WEC category [9]

Speed Range	Generator Type
0-400^{rpm}	Linear: PMSG, Rotary: Gearbox coupled, Variable speed SG / PMSG
100-250^{rpm}	Gearbox coupled, fixed speed SG / SCIG
600-1500^{rpm}	Variable speed PMSG/SCIG, Low-speed Variable-speed PMSG
1000-300^{rpm}	Variable-speed SCIG/SG/PMSG For low-storage designs: Variable-speed SG/PMSG/SCIG

types exploited in WEC systems [9]. Energy converters play a fundamental role in MEC and TEC systems. Electrical machines of the WEC branch can be classified in two subclasses: the rotary and the linear converter. PM machines are one of the brand-new rotary types which benefit from generating higher power due to the utilization of the PMs material [10]. Multiple factors impact the designating generators for MEC and TEC systems. For instance, economic and ecological aspects, generators and their drive characteristics, turbine technology, etc. Tidal currents are an exceedingly reputable source of renewable energy [11]. Customarily, convenience sites are the Bay of Fundy, Canada [12] and EMEC the Fall of Warness, UK tidal test site. Societies tend to take the advantage of renewable energy resources to solve the long-standing issues of fossil fuels concerning the rise in environmental sensitiveness [13]. A comprehensive WEC system is shown in Figure 1. At slow speeds, and by accessing the multitude of poles, on one hand, SPM benefits from an outstanding profit in terms of power density. On the other hand, the SPM generators also benefit from lower overall losses in comparison to IPM [14]. The neodymium ferrite (Nd_2Fe_{14}) corresponding to Figure 2 (a) in the proposed LS-SMPMSG, reduces the external diameter of the LS-SMPMSG which eventuates to a higher energy density, which is acceptable at low speeds. The hindrances in the utilization of Nd_2Fe_{14} could be stated as high operating temperature and considerable cost. The SPM owns higher output power, lower THD, uncomplicated and economical design, low iron loss, and ultimately, low magnet leakage flux. Accordingly, the SM-type is preferred to the LS-SMPMSG rotor. Figure 2 (b) represents the stator of the same LS-SMPMSG.

In this paper, a novel structure is proposed to design an LS-SMPMSG to be used in TEC and MEC systems. The simulation and analysis of the LS-SMPMSG have been conducted in JMAG.

2. FEM MODELLING OF LS-SMPMSG

2. 1. LS-SMPMSG Design and Assumptions In the framework of this study, a 7.2^{kW}, 100^{rpm} LS-SMPMSG has been designed. The stator is wounded by an XLPE cable with a conductor cross-section of 8 mm^2. Two layers of air and XLPE insulation, which is robust and vigorous insulation, are used to prevent any sparks in the generator. XLPE cable and the LS-SMPMSG parameters are shown in Table 2 and Table 3, respectively.

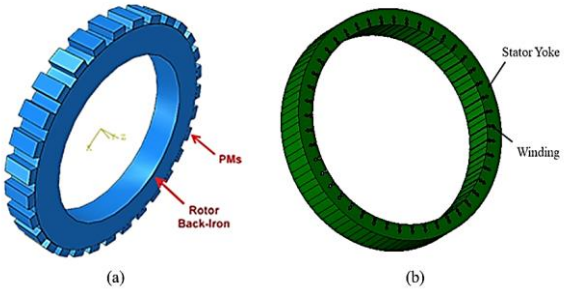

Figure 2. The LS-SMPMSG (a) rotor and (b)stator

TABLE 2. Typical properties of XLPE

Parameters	Volume
Density, g.cm^3	0.198
Tensile Strength, MPa	0.184
Elongation, %	500
Heat Distortion, %	20
Thermal Conductivity, w/m^{o}C at 90^{o}C	0.27
Modulus Elasticity, MPa	121
Dielectric Constant	2.3
Volume Resistivity, Ωm at 23°C	10^{16}

TABLE 3. LS-SMPMSG parameters

Parameters	Volume
Rated Power, KW	7.2
Speed, rpm	100
Coil Resistance, Ω	1.76
Stator Inner Radius, mm	220
Stator Outer Radius, mm	270
PM, mm	27.47×8
Cable Radius, mm	2
XLPE Insulation, mm	3.5
Air Insulation, mm	3.8
Slots/pole,-	9/3

2. 2. The LS-SMPMSG Modelling The electromagnetic field of the LS-SMPMSG is assumed as a two-dimensional problem. By combining group equations of the field and circuit, the LS-SMPMSG field equation to mode the time-dependent electrical fields are defined and described using Equation (1) [15].

$$\kappa\frac{\partial A_z}{\partial t}+\nabla\cdot\left(\nabla A_z\frac{1}{\mu_0\mu_r}\right)=-\kappa.E \tag{1}$$

where κ is electrical conductivity and μ_0, μ_r, A_z and E are the vacuum and relative permeability, the axial magnetic vector potential and applied field, respectively. In the circuit equation of the LS-SMPMSG (2)-(5), the coil end windings can be represented by coil end impedance. I_a, I_b and I_c are the conductor currents of three-phase *a*, *b* and *c*. U_a, U_b and U_c are three-phase terminal voltage obtained from solving field Eequation (1) and U_{ab}, U_{bc} and U_{cb} are the terminal line voltage between *ab*, *bc* and *ca* phases. *Rs (end)* and L_s*(end)* are coil end resistance and coil end inductance, respectively.

$$I_a+I_b+I_c=0 \tag{2}$$

$$U_{ab}=U_a+R_s(end)I_a+L_s(end)\frac{\partial I_a}{\partial t}-U_b -R_s(end)I_b-L_s(end)\frac{\partial I_b}{\partial t} \tag{3}$$

$$U_{bc}=U_b+R_s(end)I_b+L_s(end)\frac{\partial I_b}{\partial t}-U_c -R_s(end)I_c-L_s(end)\frac{\partial I_c}{\partial t} \tag{4}$$

$$U_{ca}=U_c+R_s(end)I_c+L_s(end)\frac{\partial I_c}{\partial t}-U_a -R_s(end)I_a-L_s(end)\frac{\partial I_a}{\partial t} \tag{5}$$

2. 3. The Material Used in LS-SMPMSG The materials utilized in the LS-SMPMSG are presented in Table 4. Under the appropriate operation of XLPE, the preferment of this research is to take advantages of the aforementioned insulation in the above-discussed LS-SMPMSG. In LS-SMPMSG stator used round cable winding which provides a three-phase magnetic field. Also, ArcelorMittal M800-100A and neodymium ferrite (Nd2Fe14) are used in the rotor, stator, and PM, respectively. The density of NdFeB is 7800 *kg/m*^{3}, thermal conductivity and specific heat are 7.6 *W/m/ ˚C* and 460 *J/kg/ ˚C*. The winding is a three-phase, 2 layers, and delta-connected. The range of turns in each phase is 35 and the phase resistance is *1.76* Ω. A non-uniform air gap can increase non-uniform forces in the air gap, which could lead to vibration subsequently irreversible mechanical damage to the synchronous machines. Also, based on the effect of a non-uniform air gap, the PM rotor's field is uncontrollable. Hence, a 4.5^{mm} air gap amidst the rotor and stator was chosen to avoid the non-uniform forces in the air gap and mechanical stresses. Another argument for choosing a large air gap is the ease of construction and assembly.

2. 4. Investigation of LS-SMPMSG Operation Conditions In this subsection, results of 2D analysis of the analytically designed LS-SMPMSG have been depicted. Figure 3 illustrates the LS-SMPMSG flux lines at no-load operation. Moreover Figure 4 shows the 2D flux density distribution in designed LS-SMPMSG. Figure 5 and Figure 6 indicate the Back-EMF and the three-phase stator current in the designed machine, accordingly.

TABLE 4. The material used in LS-SMPMSG

Parameters	Volume
Stator & Rotor Yoke	ArcelorMittal M800-100A
PM	NdFeB Hitachi Metals HIDENSE-500
Winding	Copper
Insulation. 1	XLPE
Insulation. 2	Air

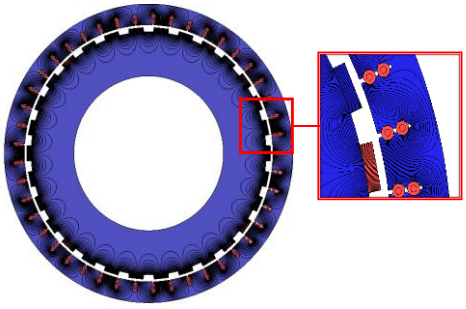

Figure 3. Magnetic flux lines of LS-SMPMSG

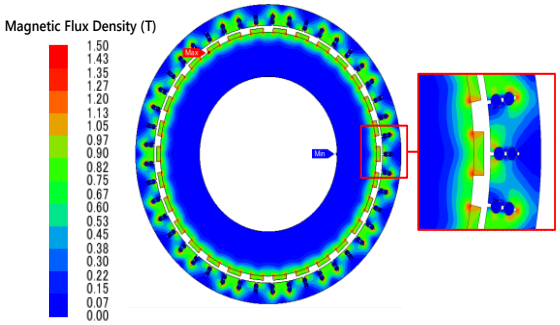

Figure 4. Magnetic flux density distribution of LS-SMPMSG

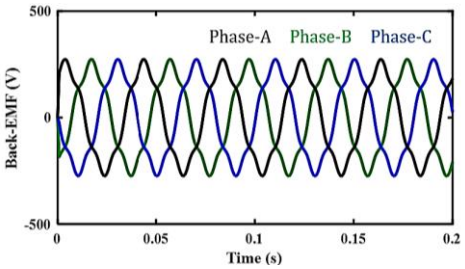

Figure 5. The LS-SMPMSG Back-EMF

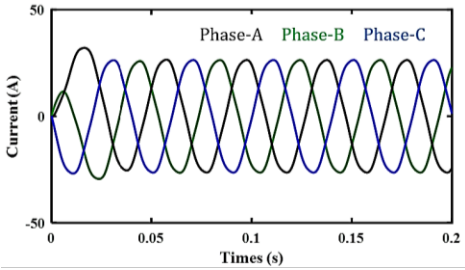

Figure 6. Three-phase stator currents in LS-SMPMSG

3. PROPOSED STRUCTURE FOR DESIGNED LS-SMPMSG

3. 1. Slot Configurations in LS-SMPMSG In this subsection, a novel slot structure for LS-SMPMSG has been proposed. The proposed scheme is facilitated in terms of LS-SMPMSG manufacture and assembly, notably its teeth and slots. In the proposed slot structure, the tooth shape has been modified and the interior space consists of cables with XLPE insulation and air gap. In the novel structure for the LS-SMPMSG, an attempt has been made to improve the previous structure. The novel proposed LS-SMPMSG slot structure is illustrated in Figure 7. As highlighted, the slot height is *W*, and five opening slots W_n are displayed. Distinct components, inclusive of the cable, XLPE insulation, air insulation, stator yoke, slot opening, air gap, and the rotor. In the last step, these five opening slot sizes are compared jointly to choose the finest opening slot. The five postures are tabulated in Table 5.

3. 2. Comparison of Five Slots Configuration In conformity with Figure 7 and Table 5, the endeavour

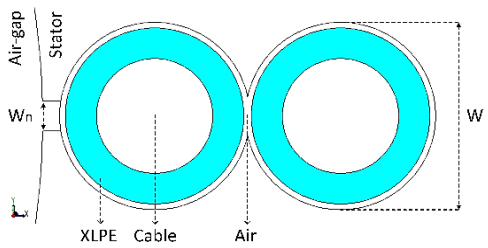

Figure 7. The proposed slot configuration for LS-SMPMSG

TABLE 5. Slot and opening slot dimensions

W_n (mm)	W (mm)	Ratio W_n / W
1	7	1/7
2	7	2/7
3	7	3/7
4	7	4/7
5	7	5/7

is to designate the incomparable opening slot for the new proposed slot configuration of the designed LS-SMPMSG. Many restrictions, such as maximum magnetic flux density, current, flux leakage, losses ordinarily Joule losses, torque, and coil inductance have been investigated to select the distinguished $W_n=1^{mm}$. Figure 8 illustrates the maximum magnetic flux density in the proposed slot configuration based on the opening slot of Table 8. In the first case ($W_n=1^{mm}$), the maximum flux density is achieved and the second state ($W_n=2^{mm}$) is the minimum. Forasmuch as the generator stator is wound, and cable is used as winding, the current passing through the stator is very indispensable. In this case, due to the shown results of Table 6, the maximum current has been obtained when the opening slot is equal to 5^{mm} which is equal to 27.17 A, and the lowest current is obtained in $W_n=1^{mm}$. The cable winding is precisely insulated with XLPE. This is one of the significant design points that should be considered in the LS-SMPMSG designing process.

The advantages of cable winding are high current and voltage tolerance. Due to the minuscule span and cross-sectional area inside the slot, the cables should be passed with great care to avoid damages to the LS-SMPMSG body and cable. Unquestionably, using the instruments for winding is the finest choice. The upper part of the slot has the same material as the LS-SMPMSG stator. This is deliberately chosen and has a positive effect on the performance of the LS-SMPMSG. In the proposed structure, in addition to having a smaller air gap, less iron is consumed. This factor has a direct impact on the weight of the machine, its manufacturing cost and its assembly cost. Joule losses, otherwise called

TABLE 6. Stator currents, Joule losses, torque and coil inductance in 5 different modes of the slot opening (W_n)

Slot Opening (mm)	Stator Currents (A)	Joule Loss (W)	Torque (Nm)	Coil Inductance (mH)
1	19.2	585.8	188.860	0.34
2	22	721.58	239.636	3.2
3	24.5	850.33	262.191	0.19
4	24.81	981	311.063	0.89
5	27.7	1071.41	343.559	4.7

RI^2 losses, are amidst the outstanding losses in the machines. One of the principal targets of such a design is to reduce losses in the machine. In agreement with Table 6, the lowest Joule losses occur in $W_n=1^{mm}$ with approximately 585.8 W. In the PM machines, the instantaneous electromagnetic torque depends on the air gap flux density waveform [16]. According to the increase in the slot opening, the torque is also increased, concerning Table 6. The findings of Table 6 exhibit that the LS-SMPMSG with $W_n=1^{mm}$ has a 188.86 *Nm* torque and increases until it reaches 343.559 *Nm* for $W_n=5^{mm}$. One of the implications which can be concluded is that a slight change in W_n leads to large changes in torque of LS-SMPMSG. Following Table 6, above all $W_n=1^{mm}$, the coil inductance is equal to 0.34×10^{-3} *H* which varies in different cases. For instance, 3.2×10^{-3} *H*, 0.19×10^{-3} *H*, 0.89×10^{-3} *H*, and 4.7×10^{-3} *H* for supplementary other four modes, respectively. To observe the changes in inductance, one of the coils is used and the diverse phases, experience the selfsame changes in the identical range of W_n alterations, according to Table 6 and also it has been found out that uneven variations of the coil inductance occur with increasing W_n. With regards to Figure 8, the maximum magnetic flux density appears in $W_n=1^{mm}$, and the minimum appears in $W_n=3^{mm}$. The high magnetic flux density gives rise to tooth saturation and it is a nuisance in the machine. According to Table 6, the stator embraces the minimum current in $W_n=1^{mm}$ and the maximum ones in the $W_n=5^{mm}$. An upward trend occurs with increasing W_n in the stator current. As it has been shown in Figure 9, the flux-linkage decreases with increasing W_n. Ultimately, the flux-linkage can be reviewing the latest significance. The $W_n=2^{mm}$ state is reduced 11.9% in comparison to $W_n=1^{mm}$, while this value between $W_n=3^{mm}$ and $W_n=2^{mm}$ is 13.5%. The comparison between $W_n=4^{mm}$ and $W_n=3^{mm}$ shows that $W_n=4^{mm}$ is 0.904 of the $W_n=3^{mm}$ and $W_n=5^{mm}$ is 0.922 of the $W_n=4^{mm}$. At last, $W_n=5^{mm}$ in comparison to $W_n=1^{mm}$ is decreased by 38.1%. In the small openings slot range, the leakage flux increases through the tooth tips which led to decreasing in flux linkage. By increasing the opening slot (W_n) at the range of greater than 4^{mm}, the flux linkage, and so, the internal machine voltage decreases. If the opening slot (W_n), not be in the proper ratio (too big or too small), the flux linkage decreases and the machine does not have its maximum rated voltage. Subsequently, like the assorted proposed slot modes, a proper opening slot should be selected as an LS-SMPMSG scheme which would be acceptable in all aspects. The opening slot (W_n) size is determined by the designer by using practical methods when manufacturing the machine. According to [17], the proper size of the opening slot for real machines is between 2.5–4^{mm} that involves numerous parameters such as the electromagnetic and the mechanical considerations of the machine. In this case, this parameter varies between 1-5^{mm} which is mostly about simulating and comparing results to determine how this parameter affects the performance of the LS-SMPMSG. This parameter has affected many parameters of the LS-SMPMSG. According to the simulation results, the proper dimension for the opening slot (W_n) is 3^{mm}. This value is a better choice that ensures the electromagnetic performance of the LS-SMPMSG and, based on this value, the improved design of the LS-SMPMSG is conducted.

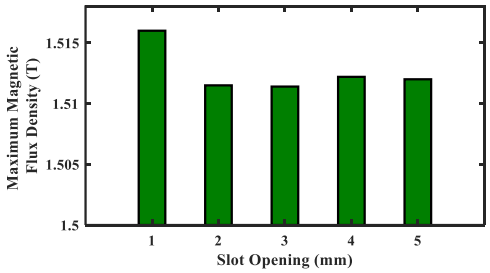

Figure 8. Distribution of maximum magnetic flux density in five different modes of the slot opening

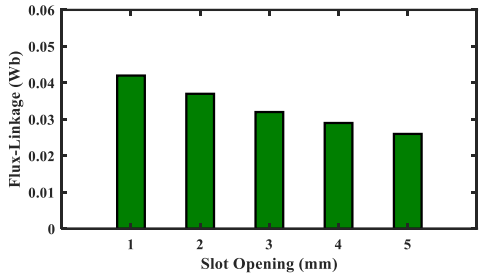

Figure 9. Flux linkage in five different modes of the slot opening

4. FEM INVESTIGATION OF THE NEW SLOT STRUCTURE

Figure 10 shows the 3D-view of the designed LS-SMPMSG with a new slot structure. In this part, the FEM analysis of the designed LS-SMPMSG is done. Figure 11 illustrates the flux line distribution of LS-SMPMSG with a new slot structure in the LS-SMPMSG stator. The stator flux density in the slot is reduced in *'New structure'*. As shown in Figure 12, the stator flux density is 1.10 *T* though in *'Old structure'* it was equal to 1.50 *T*.

5. COMPARISON BETWEEN THE NEW AND THE OLD SLOT STRUCTURE OF LS-SMPMSG

After comparing, analyzing, and examining the different structures for the opening slot, this section examines the

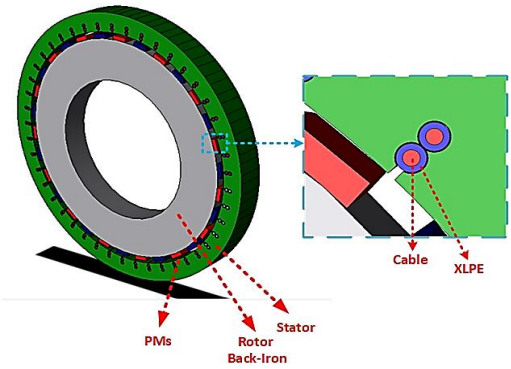

Figure 10. 3D-view of new designed LS-SMPMSG with a new slot structure

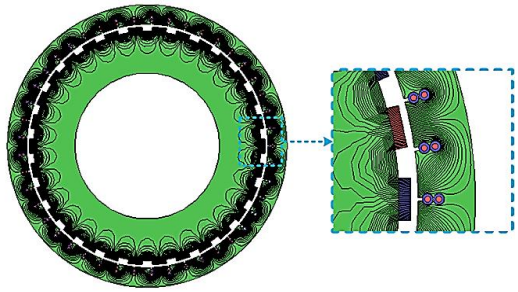

Figure 11. Magnetix flux line of new designed LS-SMPMSG with a new slot structure

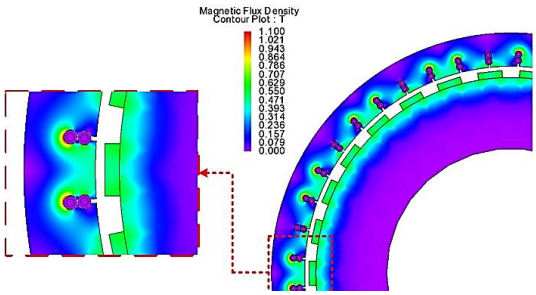

Figure 12. Magnetic flux density distribution of new designed LS-SMPMSG with a new slot structure

parameters of the new slot configuration of LS-SMPMSG with the previous ones. The previous structure with a circular slot configuration is named *'Old structure'* and the new structure with a modified slot configuration is labelled as *'New structure'*. Figure 13 shows the LS-SMPMSG torque in two forms, in the *'New structure'* the torque ripple is much less than '*Old structure'*. One more thing is the cogging torque, which depicts a significant change in the *'New structure'*. Cogging torque is a result of the interaction of PM and slots. Cogging torque, despite the torque ripples, results in noise and vibration when the machine is under load. The acoustic noise resulted from torque ripple is deleterious for the system in all cases. Changes in cogging torque are understandable in Figure 14. As it is observable, the cogging torque of the *'New structure'* has been compared to the *'Old structure'*. It is noteworthy that cogging torque has been drastically reduced by 87.5% which is a pleasant development for the *'New structure'* of LS-SMPMSG.

An extraordinarily feature of the proposed LS-SMPMSG in this paper is its slight cogging torque. In the new LS- SMPMSG structure, the design of the stator has been altered so that the redundant parts of the stator body which acts as an external air gap in the machine are eliminated. This design led to a reduction in the THD and the ripple of LS-SMPMSG torque. The significant losses are due to the Joule losses in the armature. In the *'New structure'* of LS-SMPMSG, the focus is on reducing losses, notably the Joule losses which have been demonstrated in Figure 15. In the *'New structure'* of LS-SMPMSG, the Joule losses have been

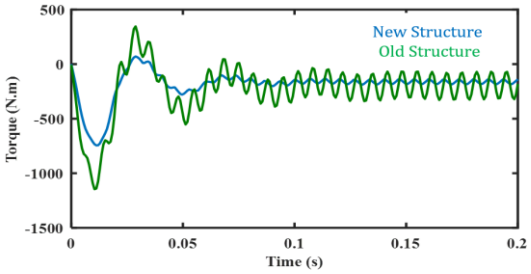

Figure 13. Torque in the *'Old structure'* and the *'New structure'* of LS-SMPMSG

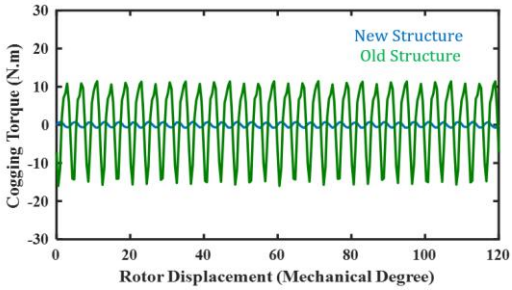

Figure 14. Cogging torque in the '*Old structure'* and *the 'New structure'* of LS-SMPMSG

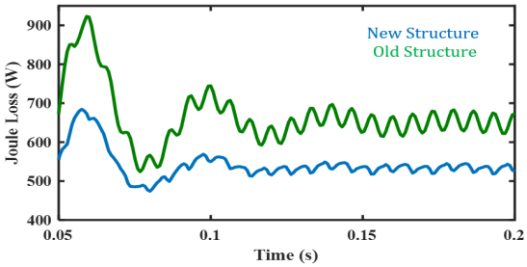

Figure 15. Joule loss in the *'Old structure'* and the *'New structure'* of LS-SMPMSG

TABLE 10. Weight in the *'Old structure'* and *the 'New structure'* of LS-SMPMSG

Old slot structure	New slot structure
292.03 Kg	291.60 Kg

diminished by 16.1%. To examine the changes made in the LS-SMPMSG, the weight of the machine has been examined for two structures. Table 10 compares the entire weight of LS-SMPMSG, proportionately. The results show that the *'New structure'* has reduced the weight of the LS-SMPMSG by 0.147%.

6. CONCLUSION

In this paper, a new slot structure has been presented based on five alternating opening slots in the LS-SMPMSG stator. The torque ripple and the cogging torque have been reduced by 19.54% and 87.5% respectively. In addition, the Joule losses and the weight of the LS-SMPMSG have been reduced by 16.1% and 0.147%, respectively. The outcomes show that the novel LS-SMPMSG slot structure proposed in this paper is very accomplishable in practice.

7. REFERENCES

1. He, C., Wu T., "Analysis and design of surface permanent magnet synchronous motor and generator,", ***CES Transactions on Electrical Machines and Systems***, Vol. 3, No. 1, (2019), 94-100. DOI: 10.30941/CESTEMS.2019.00013
2. Sun, X., Hu, C., Zhu, J., Wang, S., Zhou, W., Yang, Z., Lei, G., Li, K., Zhu, B., Guo, U., ''MPTC for PMSMs of EVs with multi-motor driven system considering optimal energy allocation,'' ***IEEE Transaction of Magnetic***, Vol. 55, No. 7, (2019), Art. no. 8104306, DOI: 10.1109/TMAG.2019.2904289
3. Shimoda, T., "A prospective observation of bonded rare-earth magnets.", ***IEEE Translation Journal on Magnetics in Japan***, Vol. 8, No. 10, (1993), 701-710. DOI: 10.1109/TJMJ.1993.4565726
4. Lin, Q., Niu, S., Fu, W. N., "Design and Optimization of a Dual-Permanent-Magnet Vernier Machine With a Novel Optimization Model.", ***IEEE Transactions on Magnetics***, Vol. 56, No. 3, (2020), DOI: 10.1109/TMAG.2019.2956071.
5. Pan, W., Li, W., Cui, L. Y., Li, X. M., Guo, Z. H., "Rare earth magnets resisting eddy currents." ***IEEE Transaction of Magnetics,*** Vol. 35, No. 5, (1999), 3343-3345. DOI: 10.1109/20.800519
6. Rahman, M. A., "History of interior permanent magnet motors [history]," ***IEEE Industry Applications Magazine***, Vol. 19, No. 1, (2013), 10–15. DOI: 10.1109/MIAS.2012.2221996
7. Patel, A.N, Suthar, B.N., "Design optimization of axial flux surface-mounted permanent magnet brushless dc motor for electrical vehicle based on genetic algorithm", ***International Journal of Engineering, Transactions A: Basics,*** Vol. 31, No. 7, (2018), 1050-1056. DOI: 10.5829/ije.2018.31.07a.07
8. Culina, J., Karsten, R., "Comparison of different resolution models and observed current profiles in the Bay of Fundy, Canada using turbine-relevant metrics," 9th European Wave and Tidal Energy Conference., Southampton, (2011). DOI: 10.1007/s00773-018-0601-z
9. O'Sullivan, D. L., Lewis, A., "Generator requirement and Functionality for Ocean Energy Converters," The XIX International Conference on Electrical Machines - ICEM 2010**.,** 1-7., (2010). DOI: 10.1109/ICELMACH.2010.5608132
10. Arish, N., Teymouri, V., "Development of Linear Vernier Hybrid Permanent MagnetMachine for Wave Energy Converter," ***International Journal of Engineering, Transactions B: Applications,*** Vol. 33, No. 5, (2020), 805-813. DOI: 10.5829/ije. 2020.33.05b.12
11. Benelghali, S., Benbouzid, M. E. H., Charpentier, J. F., "Marine tidal current electric power generation technology: State of the art and current status," 2007 IEEE International Electric Machines & Drives Conference,. (2007), DOI: 10.1109/IEMDC.2007.383635
12. Aly, H. H. H., "A novel approach for harmonic tidal currents constitutions forecasting using hybrid intelligent models based on clustering methodologies," ***Renewable Energy***, Vol 147, Part 1, (2020), 1554-1564. DOI: 10.1016/j.renene.2019.09.107
13. Fekri, H., Shamsi-Nejad, M. A., Hasheminejad, S. M., "Performance Analysis of a Novel Three-phase Axial Flux Switching Permanent Magnet Generator with Overlapping Concentrated Winding", ***International Journal of Engineering, Transactions B: Applications***, Vol. 32, No. 2, (2019), 286-295. DOI: 10.5829/ije.2019.32.02b.14
14. Vagati, A., Pellegrino, G., Guglielmi, P., "Comparison between SPM and IPM motor drives for EV application," The XIX International Conference on Electrical Machines- ICEM 2010 (2010), 1-6, DOI: 10.1109/ICELMACH.2010.5607911
15. Thomas K, Grabbe M, Yuen K, Leijon M. "A low-speed generator for energy conversion from marine currents—experimental validation of simulations" ***Proceedings of the Institution of Mechanical Engineers, Part A: Journal of Power and Energy,*** Vol. 222, No. 4, (2008), 381-388. DOI: 10.1243/09576509JPE567
16. Jahns, T. M., "Torque production in permanent-magnet synchronous motor drive with rectangular current excitation," ***IEEE Transactions on Industry Applications,*** Vol. IA-20, No. 6, (1984), DOI: 10.1109/TIA.1984.4504490
17. Fu, F. and Tang, X., *"Induction machine design handbook,"* China Machine Press, 2002, ISBN: 7-111-09078-0.

Persian Abstract

چکیده

در این مقاله به طراحی الکترومغناطیسی ژنراتور سنکرون مغناطیس دائم آهنربای سطحی سرعت پایین (LS-SMPMSG) با استفاده از روش مبتنی بر المان محدود (FEM) پرداخته شده است. ژنراتور طراحی‌شده برای استفاده در سیستم‌های تبدیل انرژی دریایی (MEC) و سیستم‌های تبدیل انرژی جزومدی (TEC) مناسب است. ویژگی اصلی LS-SMPMSG پیشنهادی، قابلیت تولید توان الکتریکی با سرعت کم در حدود ۱۰۰ دور در دقیقه است. از جمله ویژگی خاص دیگر این ساختار، استفاده از کابل به جای سیم پیچ در استاتور LS-SMPMSG است. در بخش بعدی این مقاله، یک ساختار جدید برای شیارهای استاتور LS-SMPMSG به منظور ارتقا عملکرد آن ارائه شده است. نتایج بدست آمده از روش المان محدود نشان می‌دهد که ساختار جدید منجر به کاهش ریپل گشتاور به مقدار ٪۱۹.۵۴ و گشتاور دندانه ای به مقدار ٪۸۷.۵ درصد نسبت به ساختار قبلی LS-SMPMSG شده است. این ساختار جدید همچنین بر روی تلفات ژول در LS-SMPMSG تاثیر گذاشته است به نحوی که در طراحی جدید، تلفات ژول LS-SMPMSG نسبت به حالت قبلی ٪۱۶.۱ کاهش پیدا کرده است. این پیکربندی شیار از نظر ساخت و مونتاژ شرایط را برای طراحی LS-SMPMSG مناسب‌تر کرده است. نتایج بدست آمده از روش المان محدود مزیّت های ساختار جدید پیشنهادی برای LS-SMPMSG را تایید می کند.